SMALL TO LARGE-SCALE MAPPING USING MULTI-RESOLUTION IMAGE DATA

J. Raggam, A. Almer and M.F. Buchroithner

Institute for Image Processing and Computer Graphics
Joanneum Research, Wastiangasse 6, A-8010 Graz, Austria

Commission IV

ABSTRACT

For the international high-mountain remote sensing testsite *TADAT* located in the Austrian Alps near Salzburg digital multi-resolution image data have been collected covering spaceborne Landsat-TM, SPOT and scanned KFA-1000 images as well as airborne three-line scanner images and scanned aerial photographs. An experiment was initiated to investigate the geometric performance of these different data sets in the course of *ortho-image generation* using individual images as well as *stereo mapping* based on image pairs. The geometric workstation software RSG, which is based on state-of-the-art algorithms, has been used to generate mapping products in appropriate scales from the different input images. Illustration and discussion of the basic results is given.

KEYWORDS: Mapping, Ortho-Image, Quality Control, Image Matching, Stereoscopic, 3-D

1 INTRODUCTION

The availability of digital remote sensing or photogrammetric image data in various pixel size opens the applicability of such data in cartographic work. Typical geoscientific applications are the geocoding of digital images, also known as ortho-image generation in photogrammetry, or the extraction of 3D information from digital image pairs.

An international high-mountain remote sensing testsite has been established located in the Austrian Alps near Salzburg (*TADAT*, Buchroithner and Kostka, 1989 [2]). For this, a number of digital image data in various resolutions has been collected including spaceborne Landsat-TM, SPOT and scanned KFA-1000 images, but also high-resolution airborne three-line scanner images and scanned aerial photographs.

Based on these multi-resolution image data mapping applications are presented in this paper concerning image geocoding and stereo mapping, together with a discussion of the respective results. The following objectives were treated, each of them considering *parametric mapping models* and state-of-the-art algorithms to achieve high accuracy as possible:

1. Evaluation of the geometric performance of the different image data with reference to the point transformation between image and map geometry.
2. Geocoding/ortho-image generation of image data appropriate to the image pixel size and subsequent quality control of the results.
3. Evaluation of the geometric performance of stereo pairs with reference to the image-to-map stereo intersection of projection lines.
4. Stereo mapping based on automated image correlation and a selected image pair to derive a digital elevation model (DEM).

All these activities were carried out using the remote sensing software package *RSG* (*R*emote Sensing *S*oftware Package *G*raz), which has been developed by the Institute for Image Processing and Computer Graphics (DIBAG) in particular for such geometric treatment of remote sensing data. A functional overview of this software package is given in Raggam et al. (1991, [9]) or GEOSPACE and JOANNEUM RESEARCH (1992, [3]).

2 TEST AREA AND IMAGE DATA

The *TADAT* testsite is located some 75 kilometers south-east of the City of Salzburg. It contains various topographic features ranging from high mountain peaks to a low-lying river valley, and a diversity of cultural features covering permanent icefields, cultivated land or built-up areas. For a representative part of this test area a DEM is shown in Figure 1 in an oblique view, which has been derived from topographic 1 : 25 000 maps with an initial pixel spacing of 25 meters. The following multisensor spaceborne and airborne image data have been treated:

- a *Landsat 5 TM* image with a nominal pixel size of 30 meters (denoted as TM);

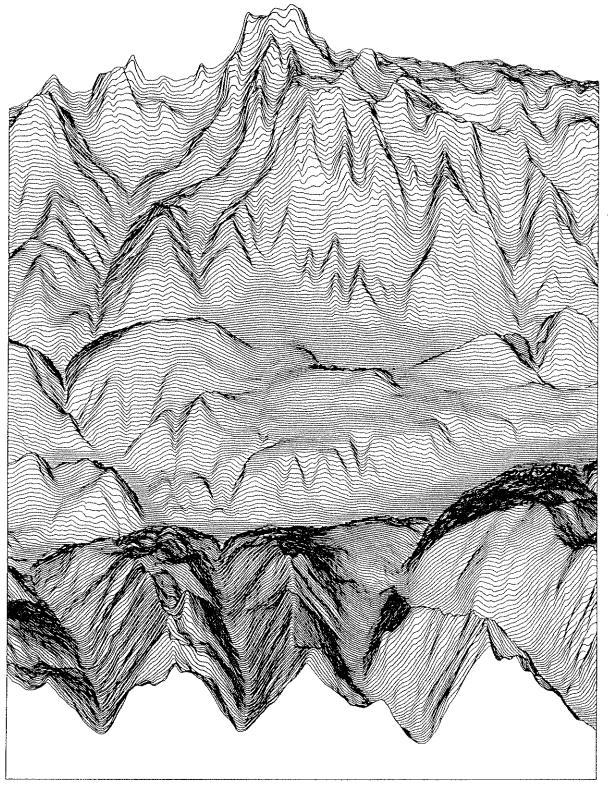

Figure 1: Axonometric oblique view of the map-derived DEM indicated in the location map.

- a *panchromatic SPOT 1* HRV-2 image with a nominal pixel size of 10 meters and nadir-looking imaging mode (denoted as SPOT);
- *KFA-1000 stereo photographs* (KFA-1, KFA-2) taken from the Sojuz space station at an altitude of approximately 285 km in a scale of about 1 : 280 000. For digital mapping, the image data were digitized with a nominal pixel size of 7 meters on ground.
- Airborne *three-line scanner imagery* using the *MEOSS* (Monocular Electro Optical Stereo Scanner, cf. Lanzl, 1986 [5]) scanner, taken at an altitude of about 11.3 kilometers, with a nominal pixel size equivalent to 2 meters on ground. Three images, denoted as MEOSS-F, MEOSS-N and MEOSS-B, are acquired from one overflight in forward-, nadir- and backward- looking mode, where the off-nadir looking angles are +/-23 degrees.
- A *scanned aerial image pair* (AIR-1, AIR-2) taken from an altitude of about 5 kilometers above ground in a scale of about 1 : 30 000, with a pixel size equivalent to about 1.5 meters on ground.

The coverage of the DEM (see Figure 1) and of the airborne image data is indicated in the location map shown in Figure 2. These only in part cover the DEM,

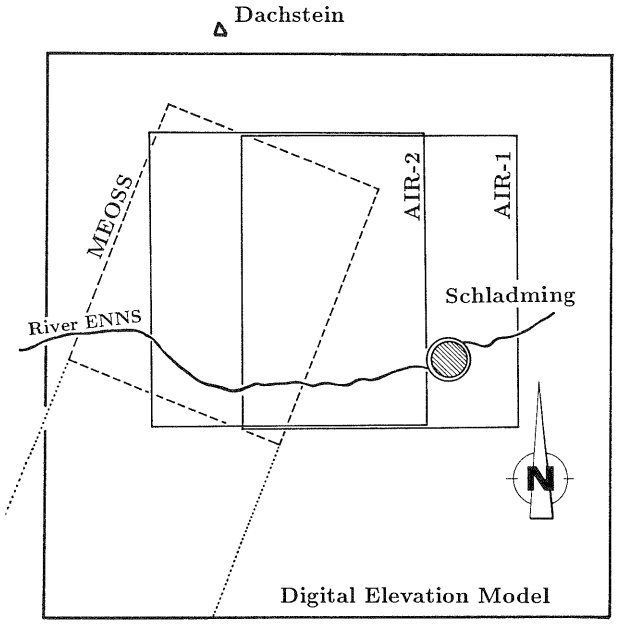

Figure 2: Topographic location map indicating the DEM and the airborne image data coverage.

whereas full coverage is available by any of the space-borne image data. Hence, subframes of this DEM have been resampled to 10, 5 and 2.5 meters, respectively, suitable for mapping purposes based on the multi-resolution image data.

Ground control points (GCPs) were measured in topographic 1 : 25 000 map sheets, in existing 1 : 10 000 ortho-photo maps and in the digital images as well. On the one hand, these points were then used to determine the geometric mapping parameters for the individual images and, on the other hand, to investigate the pointing accuracy of single images and of stereo pairs. It is obvious, that this is restricted in image and on ground by the pixel size and the scale of the reference maps, respectively.

3 DATA GEOCODING

3.1 Evaluation of Pointing Accuracy

Based on the GCPs measured on ground and in the images parametric imaging models were determined and optimized for each of the individual images using a least squares parameter adjustment implemented in the software package *RSG* (Raggam et al., 1992 [9]). Subsequently, the geometric performance of these imaging models was determined from *image residual vectors*, resulting from the transformation of control points from map geometry to the image coordinate system.

Statistical entities of these residuals can be considered as representative accuracy parameters, the re-

TABLE 1
Statistics (RMS-, Minimum-, Maximum-value) of map-to-image transformation residuals given in the image (pixels) and as nominal values on ground (meters).

Image		Along	Across	East	North
TM	RMS	0.7	0.7	21.5	20.4
	MIN	-1.8	-1.7	-50.4	-48.5
	MAX	1.4	1.8	52.3	54.6
SPOT	RMS	0.6	0.9	7.9	7.0
	MIN	-1.0	-1.7	-17.2	-15.6
	MAX	1.4	2.1	21.8	13.2
KFA-1	RMS	1.4	1.5	10.6	9.2
	MIN	-2.7	-3.4	-24.5	-18.9
	MAX	2.7	3.0	20.6	17.7
KFA-2	RMS	1.6	1.4	9.7	10.9
	MIN	-3.5	-2.8	-18.3	-20.1
	MAX	3.5	2.6	17.8	21.8
MEOSS-F	RMS	3.3	3.5	7.8	5.3
	MIN	-8.5	-8.4	-16.5	-8.4
	MAX	4.1	6.2	17.3	12.2
MEOSS-N	RMS	3.8	4.5	8.2	6.6
	MIN	-5.9	-7.7	-14.0	-11.6
	MAX	6.0	9.3	14.2	9.5
MEOSS-B	RMS	3.6	6.1	10.3	7.0
	MIN	-7.2	-10.2	-18.4	-7.6
	MAX	5.2	11.5	20.0	13.6
AIR-1	RMS	1.8	2.2	4.2	3.5
	MIN	-2.8	-4.0	-7.0	-5.6
	MAX	4.0	3.9	8.0	7.9
AIR-2	RMS	2.0	1.9	3.7	3.9
	MIN	-3.5	-2.7	-5.6	-6.8
	MAX	3.7	3.2	5.5	7.1

spective values being summarized in Table 1. This also contains the corresponding equivalents given in meters on ground, so-called *nominal residual statistics*, which are derived from simplified geometric relations. These can be considered to reflect the potential accuracy when transforming the image data to map geometry in the course of ortho-image generation.

Regarding the image pixel residuals, the RMS values are in the sub-pixel range for the Landsat TM and SPOT scanner data, whereas the accuracy achieved for the digitized KFA-1000 images is significantly worse. This may be explained by the fact, that the digitization quality of these data was rather bad and, hence, the digital KFA-1000 data by far do not show a quality comparable to the analogue data (see also Almer et al., 1990 [1]).

The Table also shows a comparatively poor accuracy for the MEOSS three-line scanner images, in particular for the across-track residual statistics. These images have been acquired in the winter season. Due to the snow coverage, but also to scanning problems – frequently entire (series of) image lines are missing – a high GCP measurement accuracy could be excluded in advance. Besides, the geometric performance of airborne scanner images may suffer from instabilities of the aircraft. More detailed studies concerning these data will be subject of future work. For the aerial images the RMS accuracy is about 2 pixels, equivalent to about 4 meters on ground, throughout and corresponds in general to the limit given by the point identification accuracy in the 1 : 10 000 ortho-photo maps.

3.2 Geocoding / Ortho-Image Generation

For the generation of geocoded images a state-of-the-art procedure as described by Raggam (1990, [7]) and implemented in the software package *RSG* was applied, which is based on the use of parametric mapping models and the integration of a digital elevation model for the compensation of terrain-induced distortions. While the Landsat TM, the panchromatic SPOT and KFA-1000 image data cover the whole reference DEM shown in Figure 1, selected subareas were resampled from this to a resolution of 2.5 meters for large-scale mapping by geocoding of the high-resolution airborne images.

Using the software package *RSG* the following geocoded products were generated:

- geocoded Landsat TM image (15 by 15 kilometers) with an initial pixel size of 25 meters, which has been resampled to 10 meters for comparison (Figure 3);
- geocoded panchromatic SPOT image (15 by 15 kilometers) with a pixel size of 10 meters (Figure 4);
- geocoded KFA-1000 images with a pixel size of 10 meters;
- MEOSS three-line-scanner ortho-images with a pixel size of 2.5 meters, a subarea (4 by 4 kilometers) of one of them being shown in Figure 5;
- aerial ortho-images with a pixel size of 2.5 meters, a subarea (4 by 4 kilometers) of one of them being shown in Figure 6.

Figure 7 shows an image mosaic in a pixel size of 5 meters, which hierarchically combines small-, medium- and large-scale image information. Here, particular image contents of Landsat TM image, SPOT image and aerial photographs simultaneously are shown, the

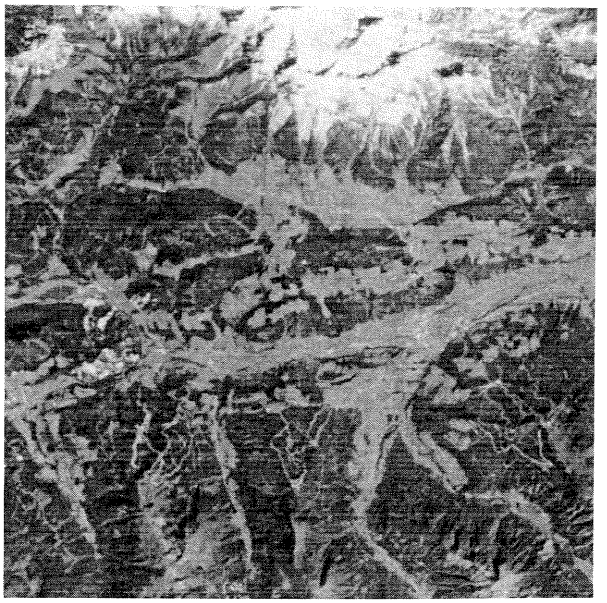

Figure 3: Geocoded Landsat TM image.

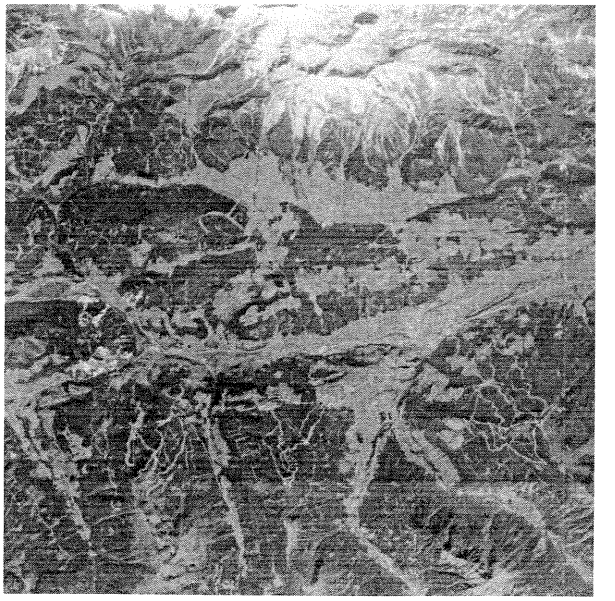

Figure 4: Geocoded SPOT image.

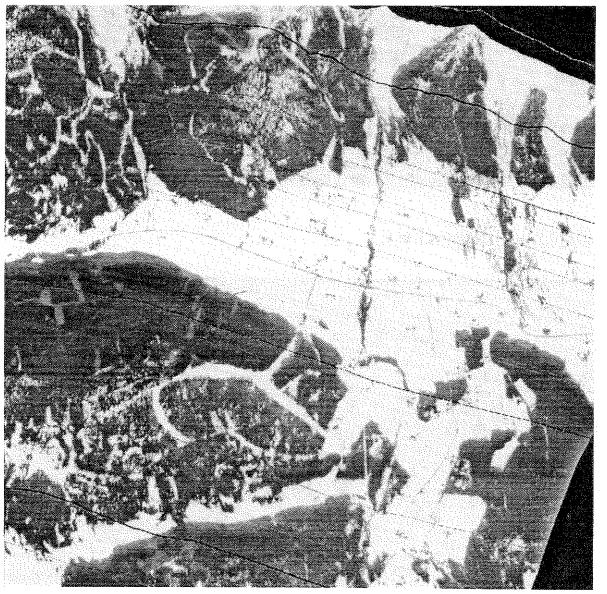

Figure 5: MEOSS three-line-scanner ortho-image.

Figure 6: Aerial ortho-image.

TABLE 2
Statistics of geocoding quality control (meters).

Image		East	North	Length
TM	RMS	16.8	20.2	26.2
	MIN	-20.7	-44.6	0.8
	MAX	34.5	35.1	44.8
SPOT	RMS	8.4	7.1	11.0
	MIN	-18.7	-13.1	1.0
	MAX	9.9	13.0	19.2
MEOSS-F	RMS	8.9	5.1	10.3
	MIN	-13.5	-9.1	1.5
	MAX	16.6	8.6	16.6
AIR-2	RMS	3.9	5.5	6.74
	MIN	-2.2	-9.1	0.3
	MAX	9.1	0.3	12.0

latter displaying settlement and built-up areas in high resolution. As illustrated, *RSG* enables to map individual subframes directly into existing geocoded images with high accuracy. The equivalent frame of a topographic 1 : 50 000 map is shown in Figure 8.

The geometric quality of the geocoded images was checked through the measurement of check points in the geocoded image frames. Respective statistical parameters on the resulting discrepancies are summarized in Table 2. As can be seen, these parameters in general show a sufficient correspondence to the nominal (a-priori) values given in Table 1. It has to be noted, that the geocoding quality statistics of the airborne images have been evaluated only for the subframes shown in Figures 5 and 6.

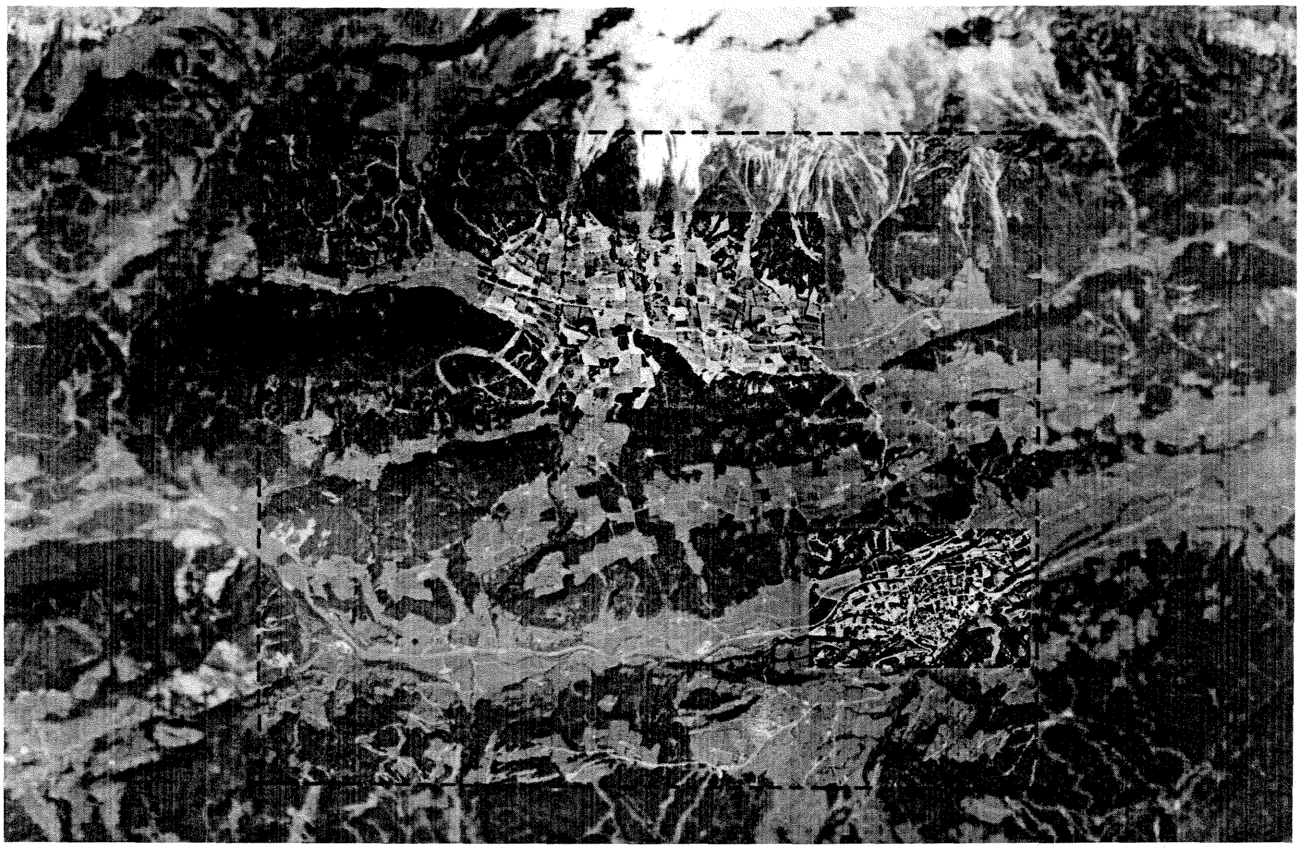

Figure 7: Mosaic of geocoded/ortho-image data.

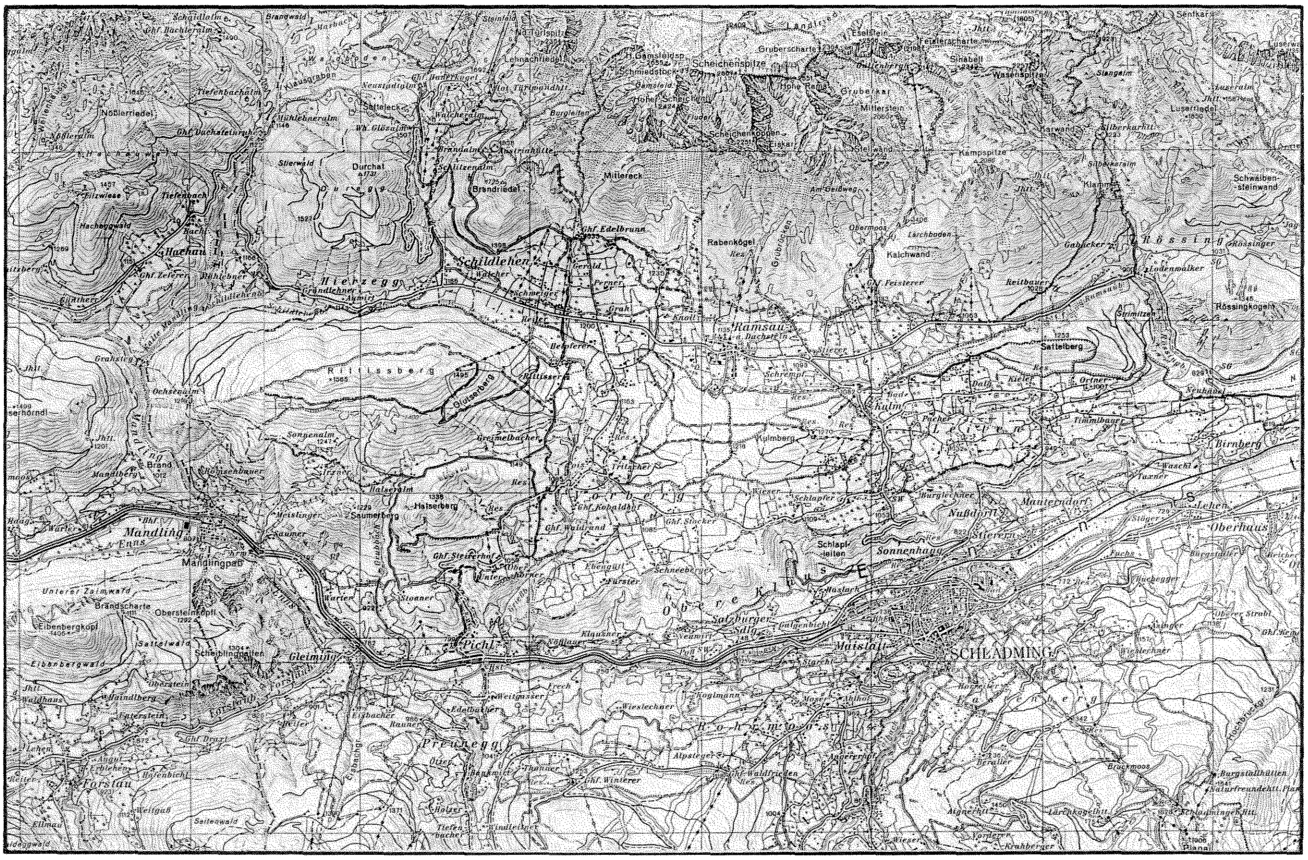

Figure 8: Cartographic frame corresponding to image mosaic.

4 STEREO MAPPING

4.1 Accuracy Assessment

The stereo mapping accuracy was derived by an image-to-map intersection of projection lines defined by the homologue coordinates of the GCPs in image geometry, so-called *epipolar lines*. This intersection results in map projection coordinates in planimetry as well as height, which can be compared to the measured coordinates of the GCPs. The resulting residuals represent the stereo model set-up accuracy and, consequently, a-priori estimates for the stereo mapping accuracy.

Statistical parameters of a-priori 3D stereo mapping residuals are summarized in Table 3 for various stereo models combined from the available image data. The software package *RSG* allows to combine individual image pairs to stereo models for further analysis without extra investment.

Concerning the KFA-1000 stereo model, the achieved values compare very well with results published by Konecny et al. (1988, [4]) or Sirkiä and Laiho (1989, [11]). While the achieved accuracy in planimetry is quite good and corresponding to the high resolution input image data, the accuracy in height is comparably poor due to the small base-to-height ratio (about 0.16) caused by the camera disposition.

As further documented, the three-line scanning mode of the MEOSS scanner basically offers a good stereo capability. Base-to-height ratios of about 0.4 and 0.8, respectively, are determined by this particular geometric imaging arrangement. For these first investigations using airborne MEOSS stereo data, however, the achieved values are worse than might be expected from this arrangement, caused again by the geometric problems mentioned in section 3. More detailed studies will be made to really exploit the stereoscopic potential of these data. A high stereo mapping accuracy of a few meters in planimetry and height is proposed by the aerial stereo model having a base-to-height ration of about 1.0. Here, general limitation is given by the GCP measurement accuracy.

4.2 Relief Mapping

The aerial stereo model was used to automatically derive a digital elevation model for a representative subarea of about 2.5 by 2 kilometers. Therefore, again the software package *RSG* was used, the algorithms implemented for stereo mapping being described in general in Raggam et al. (1991, [9]). As shown in other experiments, *RSG* offers also the possibility to combine images from different sensors for stereo mapping purposes (Raggam et al., 1991 [8], 1992 [10]).

TABLE 3
Statistics of stereo model set-up accuracy on ground (meters).

Stereo images		East	North	Height
KFA-1 / KFA-2	RMS	10.8	9.3	57.2
	MIN	-23.4	-19.4	-120.1
	MAX	19.2	18.6	106.7
MEOSS-F / MEOSS-N	RMS	10.5	7.6	17.8
	MIN	-13.0	-11.2	-33.3
	MAX	15.0	11.0	19.5
MEOSS-N / MEOSS-B	RMS	5.0	8.7	25.1
	MIN	-6.4	-10.6	-27.3
	MAX	8.2	11.7	38.9
MEOSS-F / MEOSS-B	RMS	5.9	5.5	9.1
	MIN	-9.6	-12.7	-16.3
	MAX	7.9	6.9	15.3
AIR-1 / AIR-2	RMS	4.8	4.1	8.2
	MIN	-6.0	-4.9	-8.0
	MAX	6.3	7.4	11.9

The initial processing steps have been greylevel-based image correlation and interactive measurement of homologue image points in forest areas, where no meaningful correlation output can be expected. Here, a hybrid correlation method combining greylevel- as well as feature-based approaches (Paar and Pölzleitner, 1991 [6]), together with a proper quality control, e.g. using forward-backward correlation, might reduce the interactive work.

3D coordinates were determined from homologue image point measurements through the intersection of the respective projection lines. A DEM was generated by triangulation of the received irregular point raster and subsequent interpolation of a regular elevation raster. The resulting DEM frame is shown in Figure 9 in an oblique view from South, whereas Figure 10 shows the equivalent frame of the map-derived DEM. Figures 11 and 12 show the corresponding contour lines (contour interval 20 meters) and Figure 13 shows an overlay of the stereo-derived DEM and a geocoded aerial image.

Using *RSG*, statistical parameters for the height differences have been determined, resulting in a standard deviation of 9.7 meters. This corresponds well to the a-priori height accuracy of 8.2 meters given in Table 3. Also a visual comparison of Figures 9 and 10 shows a good correspondence of the DEMs at least in those areas, where meaningful stereoscopic measurements can be made.

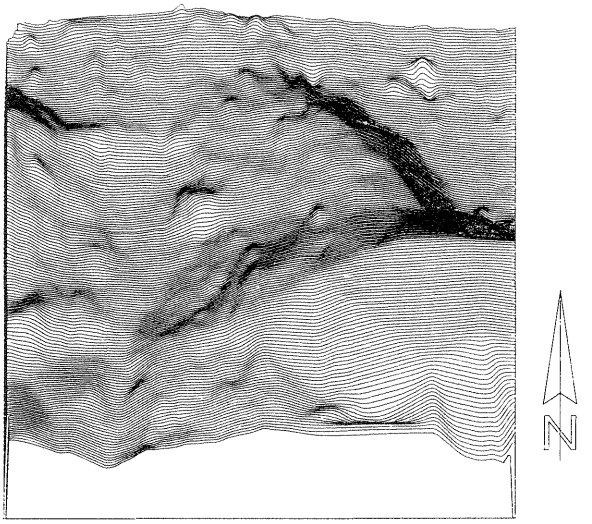

Figure 9: Oblique view of stereo-derived DEM.

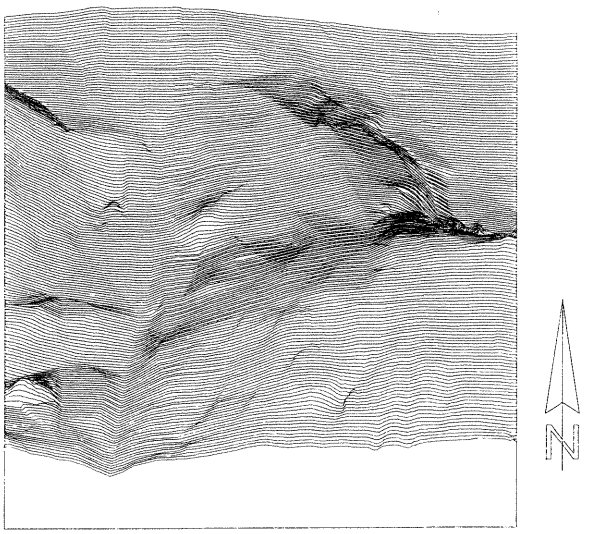

Figure 10: Oblique view of map-derived DEM.

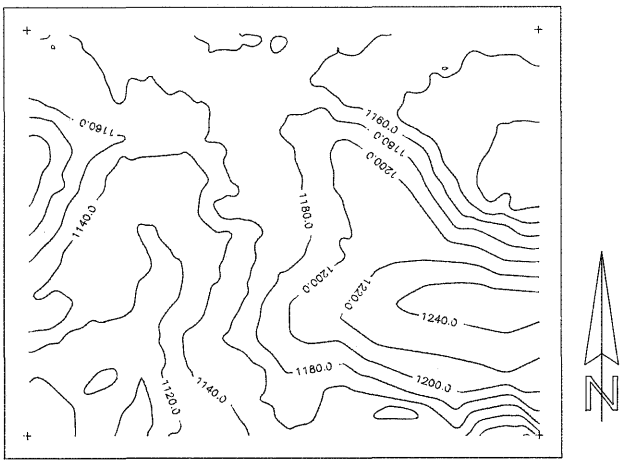

Figure 11: Contour lines of stereo-derived DEM.

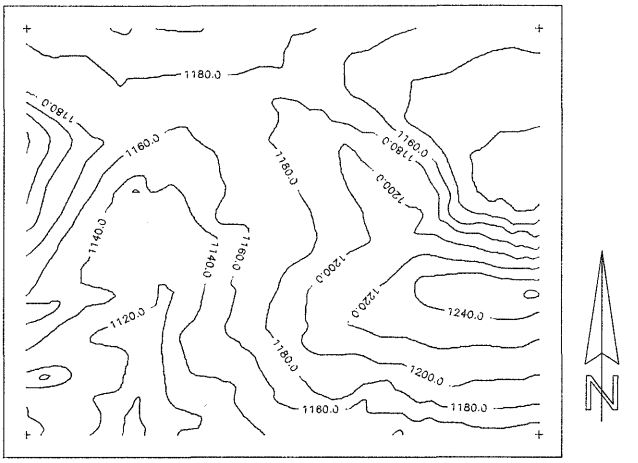

Figure 12: Contour lines of map-derived DEM.

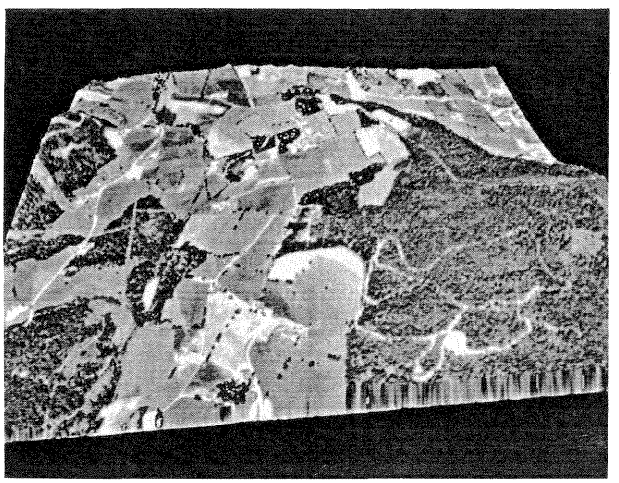

Figure 13: Superposition of stereo-derived DEM and geocoded aerial image.

5 CONCLUSIONS

Investigations into the potential of mapping in small and large scales using multiple scale image data have been carried out in the presented study. Geocoded images have been generated from the image data at appropriate pixel resolution and compared to available cartographic data like topographic maps or orthophoto maps. Basically, the accuracy of this image-to-map transformation is limited by the pixel size, i.e. the scale, of the input image data. Hence, an interaction of this parameter and a reasonable cartographic scale of the output product is given.

For a small scale Landsat TM image a mismatch on ground equivalent to about 0.2/0.1 millimeters in topographic 1 :100 000/1 :200 000 maps was determined. Medium scale image data, in particular panchromatic

SPOT data, show a mapping accuracy equvalent to 0.3/0.15 millimeters in 1 : 25 000/1 : 50 000 maps. Map revision at large scales of 1 : 10 000 becomes feasible using scanned aerial photos. For these data accuarcy limitation is given by the image scale and by the scanner performance. In the presented applications, a mapping accuarcy corresponding to about 0.2 millimeters in 1 : 10 000 scale could be achieved.

Digital image data also offer a certain potential for 3D data extraction. Digitized aerial photographs are a subject in digital photogrammetry, which offers the possibility of automated stereo mapping based on image correlation techniques. An activity for DEM extraction using such data has been carried out. Compared to existing elevation data derived from 1 : 25 000 topographic maps the resulting DEM shows more details in particular areas. However, for individual homogeneous areas like forests automatic image correlation is not possible. There, miscorrelations can lead to rather erroneous results. It is a matter of further investigations to identify methods to appropriately avoid miscorrelations.

REFERENCES

[1] A. Almer, M. F. Buchroithner and J. Raggam (1990):
Digital Mapping with High Resolution Sojuz KFA-1000 Images. In *Proc. of 10'th EARSeL Symposium: New European Systems, Sensors and Applications*, pp. 403–417, Toulouse, France, June 5-8 1990.

[2] M. F. Buchroithner and R. Kostka (1989):
TADAT - an International Alpine Test Site for Remote Sensing Data. In *Proceedings of the 9th EARSeL Symposium*, Espoo – Finland, 27 June - 1 July 1989, pp. 306 - 310.

[3] GEOSPACE and JOANNEUM RESEARCH (1992):
Remote Sensing **S**oftware Package **G**raz – Software for Geometric Treatment of Multisensor Remote Sensing Data. *Colour Brochure*, 10 pages.

[4] G. Konecny, K. Jacobsen, P. Lohmann and W. Müller (1988):
"Comparison of High Resolution Satellite Imagery for Mapping", *International Archives ISPRS*, Kyoto – Japan, Commission IV, Vol. 27, Part B 9, pp. 226 - 237.

[5] F. Lanzl (1986):
The Monocular Electro-Optical Stereo Scanner (MEOSS) Satellite Experiment. *International Archives of Photogrammetry and Remote Sensing*, Vol. 26-1, pp. 617 - 620, Stuttgart.

[6] G. Paar and W. Pölzleitner (1991):
Automatic 3D Modelling by Pyramid-Based Stereovision Using Remotely Sensed Data. In Proc. *Modelling and New Methods in Image Processing and in Geographical Information Systems*, Oldenbourg-Verlag, Vienna-Munich, ed. by P. Mandl, Klagenfurt, April 1991.

[7] J. Raggam (1990). "Interpolative Map-to-Image Coordinate Transformation for Spaceborne Imagery", in *Proceedings of the IGARSS 1990 Symposium: Remote Sensing - Science for the Nineties*, Vol. II, pp. 1423 - 1426,Washington D.C.

[8] J. Raggam and A. Almer (1991):
A Multi-Sensor Stereo Mapping Experiment. *ACSM/ASPRS/Auto Carto Annual Convention*, Vol. 4, pp. 173 - 182, Baltimore, Maryland, March 1991.

[9] J. Raggam, D. Strobl, M.F. Buchroithner and A. Almer (1991):
RSG – Workstation Software for Geometric Multisensor Data Processing. In *Proc. "Digital Photogrammetric Systems"*, Wichmann-Verlag, Munich, Germany, ed. H. Ebner, D. Fritsch, Ch. Heipke, pp. 313 - 325.

[10] J. Raggam, A. Almer and D. Strobl (1992):
Multisensor Mapping Using SAR in Conjunction with Optical Data. In *International Archives ISPRS*, Washington D.C., Commission II, 1992.

[11] O. Sirkiä and A. Laiho (1989):
"An Investigation of the Geometric Properties of the Sovjet KFA-1000 Space Images", in *The Photogrammetric Journal of Finland*, Vol. 11, No. 2, pp. 74 - 83.